Metastable Secondary Structures in Ribosomal RNA Molecular Hysteresis in the Acid–Base Titration of *Escherichia coli* Ribosomal RNA

Arnold Revzin†, Eberhard Neumann‡ and Aharon Katchalsky§

Polymer Department, The Weizmann Institute of Science, Rehovot, Israel

The metastable conformational states which underlie the hysteresis displayed by *Escherichia coli* ribosomal RNA in its pH titration in the acid range have been analyzed in terms of acid-stable RNA secondary structures. Sedimentation measurements show that the phenomenon is *intra*molecular, so that analysis of the hysteresis loops can, in principle, reveal details of molecular architecture. Hysteresis cycles obtained spectrophotometrically and potentiometrically were compared for RNA in solutions of different ionic strengths and ionic compositions. The effect is much smaller at lower ionic strength and disappears in the absence of magnesium ions. The curve followed upon addition of acid appears to reflect the equilibrium state of the system at each pH value. On the "base branch" of the loop, a slow absorbance change (complete in hours) was observed after the pH was raised by addition of a portion of base. This slow process is attributed to the annealing of "mismatched" multihelical regions of the ribosomal RNA. Certain regions, however, remain in metastable configurations for days and it is these long-lived non-equilibrium structures that underlie the hysteresis. Titration at 35°C gave hysteresis loops of the same size and shape as at 20°C; indeed, we found that the metastabilities are not removed even at 80°C. Ultraviolet light absorbance difference spectra at 80°C between solutions at the same pH, but on different branches of the cycle, give insight into the nature of the metastable conformation(s).

Our experimental observations lead us to propose that the hysteresis is due to the formation at acidic pH of double-helical structures involving protonated guanine and adenine base pairs. The G·G pairs seem especially important to account for the very high thermal stability, as well as for the fact that the structures formed at a given pH value as acid is added dissociate only at higher pH values when the solution is titrated with base. Titrations of transfer RNA, along with literature data on 16 S rRNA primary structure, imply that the metastable regions in rRNA may consist of perhaps 10 to 15 base pairs.

1. Introduction

An unusual feature of certain ribosomal RNAs is the existence of true hysteresis phenomena in their pH titrations in the acid range (Everett, 1967; Cox & Littauer, 1963; Cox, 1966; Cox & Katchalsky, 1972). That is, the optical density (or proton

† To whom correspondence should be addressed at the Institute of Molecular Biology, University of Oregon, Eugene, Ore. 97403, U.S.A.

‡ Present address: Max-Planck-Institut für biophysikalische Chemie, D-34 Göttingen, Germany.

§ This work was initiated under the guidance and inspiration of the late Aharon Katchalsky. We regret that the final form of the manuscript did not benefit from his critical insight and comments.

binding) *versus* pH data lie on one curve when the pH is lowered by addition of acid, and on a different curve when the pH is raised by addition of base. One obtains a closed loop, which can be reproduced on successive titration cycles. The loop exists between definite pH limits, while above and below these limits only a single reversible curve is observed. "Scanning" curves (Everett, 1967; Cox & Katchalsky, 1972) and loops within the main loop can also be obtained.

Hysteresis loops for rRNA reflect the presence of long-lived metastable conformational states and non-equilibrium transitions in the system (Cox & Katchalsky, 1972). We shall show that the phenomenon is an intramolecular one so that analysis of the hysteresis can in principle yield information about the structure of individual RNA molecules. It is generally accepted that at pH 7 rRNA is composed of a series of double-helical domains (of from 4 to 20 base pairs) separated by single-stranded regions (containing about 3 to 10 residues) (Doty *et al.*, 1959; Cox, 1966; Spirin & Gavrilova, 1969). The double-helical regions are probably of the Watson–Crick type (Timasheff *et al.*, 1961; Arnott *et al.*, 1966). It seems likely that at lower pH values there may be rearrangements to different types of base-paired regions, and we may infer which structures are likely by considering the properties of model polynucleotides.

Cox & Katchalsky (1972) have discussed rRNA hysteresis qualitatively by using a hypothetical nucleotide sequence devised by Cox (1966). This hypothetical sequence has the same over-all base composition as rRNA, and the arrangement of the residues allows the formation of acid-stable regions at low pH values. All features of the real hysteresis cycle, such as the smooth loop and the existence of scanning curves, were interpreted in terms of possible conformations of the hypothetical RNA. Cox & Katchalsky (1972) observed that the hysteresis may well be due to the prevention of the nucleation step in the formation of a (equilibrium) double-helical region; the barrier could arise because of metastability in the "low pH" structures which prevents nucleation by immobilizing the appropriate bases in non-equilibrium configurations.

A quantitative analysis of RNA titration behavior, based on extensive new u.v.-absorbance and proton-binding data, will be given in another paper (Revzin, Neumann & Katchalsky, manuscript in preparation). The primary goal of the current study was to ascertain which of the conformations that RNA regions can assume in solution may be metastable and thus underlie the hysteresis.

2. Materials and Methods

(a) *Materials*

The rRNA was a mixture of 16 S and 23 S particles prepared from fresh 70 S *E. coli* ribosomes (strain MRE600) which were a gift from Dr D. Elson. The ribosomes were isolated using the protocol in Spitnik-Elson & Atsmon (1969), and the nucleic acid was extracted following the sodium dodecyl sulfate–phenol procedure described by Eilam & Elson (1971). After treatment with dodecyl sulfate, the RNA was purified by extraction 2 or 3 times with phenol and chloroform. After precipitation from distilled ethanol containing 2% potassium acetate, the RNA was dialyzed against several changes of sterile distilled water. The dialysis bags had been sterilized by autoclaving. The concentrated RNA solution was lyophilized and the dry RNA stored in small portions at −20°C. Nucleic acid solutions for titration were prepared from individual small portions of dried material immediately before starting experiments. The integrity of the RNA, as judged

from sedimentation boundary analysis, was maintained even after several freezing–thawing cycles. All RNA solutions were slowly filtered through sterile Millipore filters. Lowry analysis showed that residual protein was less than 1%. The preparation procedure described above was used to prepare two large batches of rRNA.

Transfer RNA (mixture from *E. coli* strain K12W6, T_1 ribonuclease free) was a gift of Dr U. Z. Littauer.

(b) *Buffers*

Buffers were prepared from analytical grade reagents used without further purification. All buffer solutions were autoclaved before use. Strict sterility was observed in preparation and handling of solutions and glassware. Sterile water was obtained by autoclaving water which had been doubly distilled from permanganate. Absorbance cuvettes were sterilized by immersion in 6 N-HNO_3 for 5 to 10 min followed by thorough rinsing with sterile water. Glassware was treated either by the nitric acid process or by heating at 160°C for several hours. New plastic gloves were worn whenever relevant. Experiments in which these precautions were not observed inevitably resulted in failure.

(c) *Potentiometric titrations*

Potentiometric titrations were performed with a Metrohm EA147 combined microelectrode and a Radiometer pH meter 26, using a cell of special design, which minimized the risk of bacterial contamination while permitting the electrode and the titrants to be easily introduced. The vessel was immersed in a water bath, and stirring was effected magnetically. A nitrogen atmosphere was maintained above the surface of the solution to prevent CO_2 absorption. The electrode was sterilized immediately before use by dipping it several times into 6 N-HNO_3 and rinsing with sterile water; tests showed that this had no adverse effect on electrode performance.

Approximately 10·5 ml of solution, having an RNA concentration about 4×10^{-3} M-[P]†, were titrated in each experiment. The ionic composition of the solution was 0·099 M-NaCl, 0·001 M-sodium cacodylate. The exact amount of solution was determined by weighing the vessel before and after filling. The phosphate concentration was determined spectrophotometrically, using an extinction coefficient for RNA, $\epsilon_{260} = 7450$ cm^{-1} M-[P]$^{-1}$ ($T = 20°C$, wavelength, $\lambda, = 260$ nm) (Littauer & Eisenberg, 1959). For these measurements, 50 or 100 μl RNA solution were diluted into a weighed amount (about 2·5 ml) of buffer. A "blank" solution, containing buffer, but not RNA, was titrated in each experiment.

Acid (HCl) and base (NaOH) were 0·1 M and were added from Agla syringes with Teflon needles; the syringe calibrations were checked against weighed amounts of standard phthalate solution. (Some problems were encountered with evaporation from the junctions between syringe parts—this was reduced to a tolerable level by sealing the exposed parts of the syringes with a light grease.)

After sufficient titrant was added to change the pH by about 0·25 unit, the pH was recorded as a function of time. No significant drifts in pH were observed. It should be noted that any changes in pH due to uptake or release of protons *via* a slow reaction of the RNA would have been masked at high pH by the presence of 0·001 M-sodium cacodylate buffer and at low pH by the buffering capacity of the solvent itself.

(d) *Spectrophotometric titrations*

Spectrophotometric titrations were performed in a Zeiss PMQII spectrophotometer. The pH was determined simultaneously with the absorbance by placing a Metrohm combined microelectrode in the cuvette, out of the light path. The electrode was sterilized immediately before use, as described above. Temperature was controlled with a Zeiss thermostatically controlled cell block. Titrants were added from Agla microsyringes fitted with long Teflon needles and stirring was achieved by a Zeiss stirring motor unit combined with a small magnetic stirrer in the cuvette. After sufficient titrant was added to change the pH by the desired amount (usually 0·2 to 0·5 pH unit) the absorbance spectrum was

† Abbreviation used: [P] denotes phosphate residues of the polynucleotide backbone.

read at appropriate time intervals until no further change in absorbance with time was observed. The RNA concentration was about 10^{-4} M-[P] for these experiments.

(e) *Sedimentation measurements*

Sedimentation coefficients were determined with a Beckman model E ultracentrifuge, equipped with u.v.-absorbance optics and a photoelectric scanner. The RNA solutions were the same as those used in the spectrophotometric titrations ([P] $\sim 10^{-4}$ M). Measurements were taken at a rotor speed of 32,000 revs/min and the rotor temperature was maintained at 20°C.

(f) *Absorbance difference spectra at 80°C*

Absorbance difference spectra for two RNA solutions at the same pH but on different branches of the hysteresis loop were determined over the temperature range 20 to 80°C. About 2·5 ml of freshly prepared RNA solution (10^{-4} M-[P], 0·099 M-NaCl, 0·001 M-sodium cacodylate, 2×10^{-4} M-MgCl$_2$, pH 7), were transferred to each of two spectrophotometric cuvettes (of about 4 ml capacity). A solution on the "acid branch" was obtained by titrating the material in one cuvette with acid directly to the pH of interest (e.g. pH 4·0), then adding 50 μl of sodium acetate–acetic acid buffer (0·1 M in Na$^+$) to control the pH at the desired value. The material in the second cuvette was titrated with acid to pH 3·0 or 2·8 (titration time about 15 to 30 min); after 10 to 15 min at the low pH, base was added slowly to bring this "base branch" solution to pH 4·0, and 50 μl of buffer were added. The optical density was monitored throughout each titration. The solutions were then left for at least 10 h to be certain that slow changes in absorbance with time (especially for the base branch solution) had levelled off. (It was thus possible to check that we had successfully produced solutions at the same pH on the acid and base branches of the hysteresis loop, a necessary precaution since for unknown reasons titrations occasionally ended in failure.) About 1 ml of each of the two solutions was transferred to smaller cuvettes. These cuvettes, loosely stoppered, were placed in a thermostatically controlled cell block and heated to about 80 to 85°C using a Haake temperature regulator. The absorbance of each solution was read at approximately 10 deg. C intervals while heating and cooling. The highest temperatures were maintained for as short a time as possible to minimize degradation of the RNA. Total time for a heating–cooling cycle was 2 to 2·5 h. Cuvettes were weighed before and after heating—losses due to evaporation were less than 0·5%. Some experiments were performed by placing the cells in a cell block preheated to the desired temperature, reading the absorbance after equilibration, then rapidly cooling the solutions to 20°C.

The effect of EDTA on acid and base branch solutions was checked by preparing such solutions at pH 4 and then adding excess EDTA to a final concentration of about 5×10^{-3} M. After slow absorbance changes had levelled off, absorbance difference spectra were determined for these solutions at elevated temperatures and also upon recooling.

3. Results

(a) *Potentiometric titrations*

The results of the potentiometric titrations are presented in Figure 1. As noted in the Introduction, the base branch curves followed upon titration with base from low pH do not coincide with the acid branch curve obtained when titrating with acid from pH 7. Addition of acid to a solution which has undergone a full titration cycle gives a curve which is coincident with the first acid branch. This indicates that after the hysteresis cycle has been completed the RNA has returned to its original (pH 7) configuration.

The number of protons bound was calculated by considering the difference in amount of titrant needed to bring the nucleic acid and "blank" solutions to the same pH value (Tanford, 1962, p. 76). Since a study of the hysteresis phenomenon requires
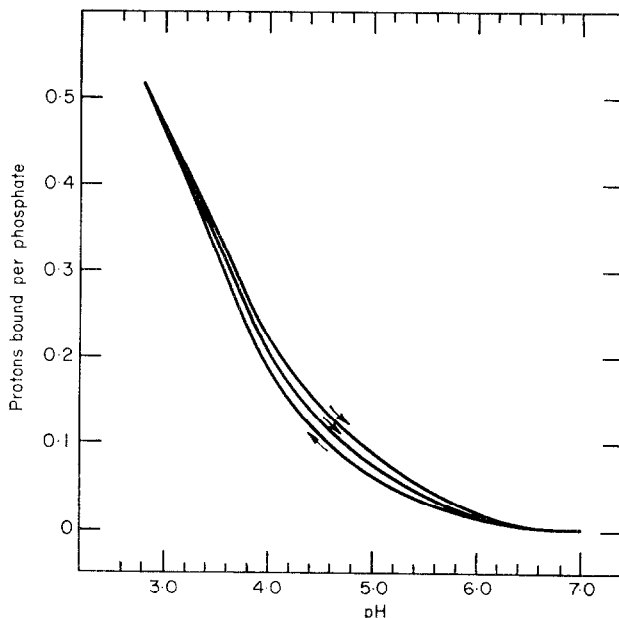
FIG. 1. Potentiometric titration of unfractionated *E. coli* rRNA. Experimental conditions: $T = 20°C$; buffer, 0·099 M-NaCl, 0·001 M-sodium cacodylate; RNA concentration, ~4 × 10⁻³ M-[P]. These data were derived using RNA from our first preparation (see text) which apparently contained sufficient residual Mg^{2+} to show the full hysteresis effect. The three curves are: lower curve, acid branch; upper curve, base branch from pH 2·8; middle curve, scanning curve from pH 3·2.

more than one acid–base cycle to be performed on a single solution, the computations require more extended relations than is usually the case. We denote the nucleic acid solution by a superscript N and the "blank" by a superscript B, and we let V_H^i, V_{OH}^i be the volumes of acid (molarity M_H) and of base (molarity M_{OH}), respectively, added to solution i. Also, let V_0 be the initial volume of each (pH 7) starting solution. If we make the good assumption that the activity coefficient of H^+, γ_{H+}, at a particular hydrogen-ion concentration is independent of the presence of nucleic acid, then when the RNA and the blank solutions have the same pH, the general equation for the number of protons bound, Δn, is

$$\Delta n = \frac{1}{V_0 + V_H^B + V_{OH}^B} \tag{1}$$
$$[V_0 M_H(V_H^N - V_H^B) - V_0 M_{OH}(V_{OH}^N - V_{OH}^B) - (M_H + M_{OH})(V_H^B V_{OH}^N - V_H^N V_{OH}^B)].$$

Note that $\Delta n = 0$ for the starting solution.

On the first acid branch of the titration, $V_{OH}^B = V_{OH}^N = 0$, and the number of protons bound at any pH is

$$\Delta n = \frac{1}{V_0 + V_H^B} [V_0 M_H (V_H^N - V_H^B)], \tag{2a}$$

where V_H^N and V_H^B are the volumes of acid needed to bring the two solutions to that pH value.

Calculations for the base branch are simplified if the same volume of acid is added to each solution before base is added. This makes $V_H^N = V_H^B$ at each point on the base branch, and

$$\Delta n = \frac{1}{V_0 + V_H^B + V_{OH}^B} [V_0 M_{OH} + V_H^B(M_H + M_{OH})] \cdot (V_{OH}^B - V_{OH}^N), \qquad (2b)$$

V_{OH}^N and V_{OH}^B being the volumes of base added to bring the two solutions to the pH of interest. Similarly, before adding acid again equal volumes of base are added to each solution. Then, for the second acid branch we have

$$\Delta n = \frac{1}{V_0 + V_H^B + V_{OH}^B} [V_0 M_H + V_{OH}^B(M_H + M_{OH})] \cdot (V_H^N - V_H^B). \qquad (2c)$$

Equations for subsequent base or acid branch titrations on the same solution can be written by inspection, using the above equations as guides.

Equations (2a) to (2c) are virtually exact expressions that facilitate rapid calculation of Δn. We have computed Δn by comparing the nucleic acid and blank solutions at the same pH value (rather than using differences in pH for "N" and "B" solutions to which equal volumes of titrant have been added). Our procedure eliminates the need to know the value of γ_{H+}, and also minimizes any liquid junction potential or glass electrode correction differences between the two solutions (Steinhardt & Beychock, 1964, p. 158).

Values for Δn computed using equations (2a) to (2c) were converted to H^+ bound per phosphate (denoted by $H^+/[P]$) using the concentration determined by procedures described under Materials and Methods.

(b) Spectrophotometric titrations

The results of the spectrophotometric titrations are presented in Figures 2 and 3. The u.v.-absorbance, A_λ, was recorded at six wavelengths, and was corrected for dilution from addition of titrant. For the sake of comparison, absorbance readings were all converted to those for an equivalent solution of nucleotide concentration 10^{-4} M-[P]. Different experiments gave loops which were reproducible in size and shape to ± 0.004 absorbance unit. Figures 2 and 3 show both the boundary loops of the hysteresis cycle and selected scanning curves. Scanning curves are obtained from both branches of the loop. The acid branch is reversible to pH 3.8 (i.e. the hysteresis is seen only if the back titration is started from pH < 3.8).

It is difficult to determine accurately the actual point of closure of the loops as higher pH is reached upon titration with base. Even small increases in absorbance, due perhaps to limited hydrolysis of the RNA (Cox, 1968) can displace the closure point by, say, 0.5 pH unit. It is found that the loops are closed somewhere between pH 5 and pH 6. As in the potentiometric titrations, after a cycle was completed the system followed the lower curve upon further addition of acid, indicating that the RNA had returned to its initial pH 7 configuration.

(c) Time independence of hysteresis loops

Figure 4(a) represents the low pH section of a spectrophotometric titration cycle at $I = 0.1$ M (in the presence of Mg^{2+} ions, see below). Let us consider the addition of base to a solution at point P (say, at pH 3.5) on the base branch of the loop. The
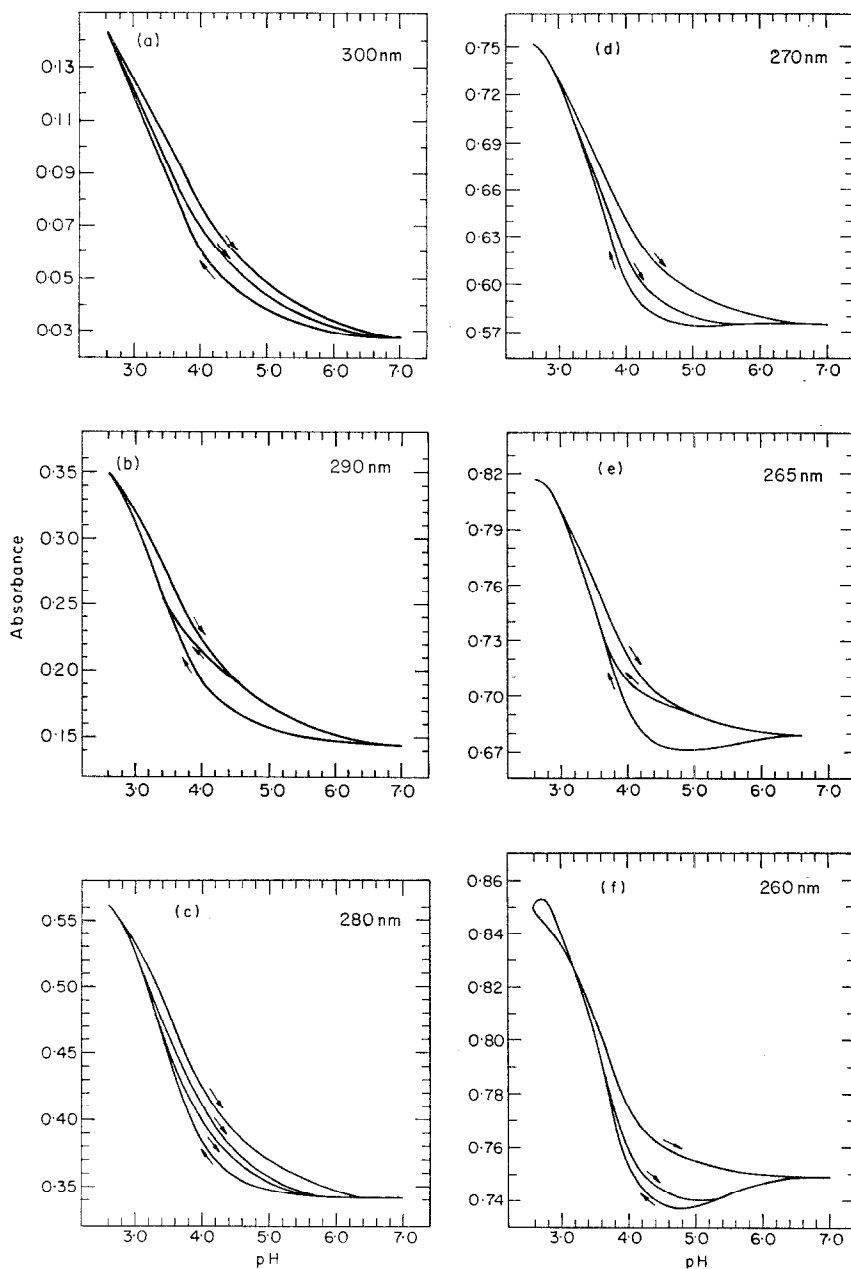
FIG. 2. Spectrophotometric titration of unfractionated *E. coli* rRNA. Experimental conditions: $T = 20°C$; buffer, 0·099 M-NaCl, 0·001 M-sodium cacodylate, $\sim 2 \times 10^{-4}$ M-MgCl$_2$. (Identical curves were obtained with our first RNA preparation, without the addition of Mg^{2+} ions (see text).) All data have been converted to a standard RNA concentration of 10^{-4} M-[P]. For each of the six wavelengths shown, the lower curve is the acid branch of the hysteresis loop and the upper curve is the base branch from pH 2·6. Intermediate curves are selected scanning curves from the acid or base branches. No hysteresis is observed unless the pH is decreased below pH 3·8. Curves are for time-independent absorbance readings (see text).
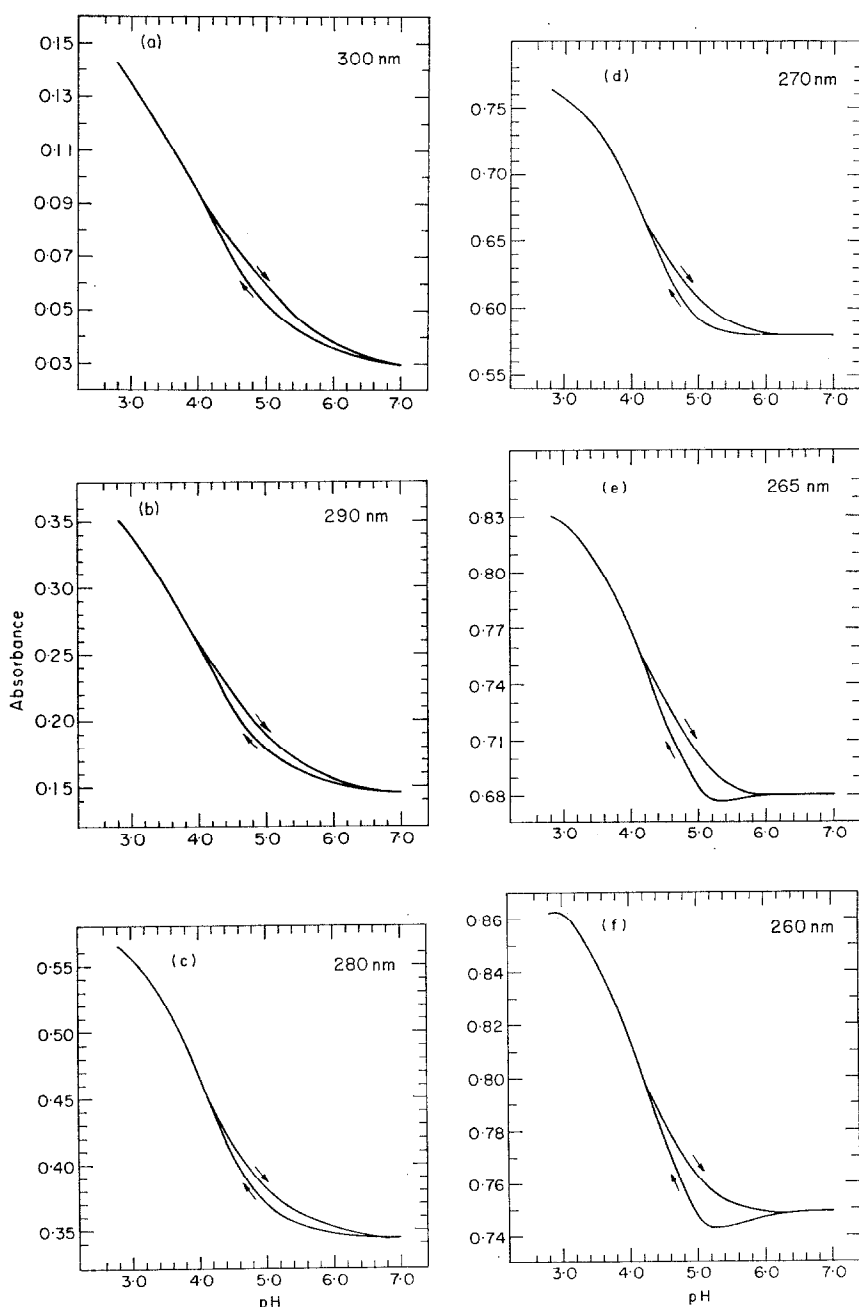
FIG. 3. Spectrophotometric titration of unfractionated *E. coli* rRNA. Experimental conditions: $T = 20°C$; buffer, 0·009 M-NaCl, 0·001 M-sodium cacodylate. These data were derived using RNA from either preparation, without addition of Mg^{2+} ions. All data have been converted to a standard RNA concentration of 10^{-4} M-[P]. For each of the six wavelengths shown, the lower curve is the acid branch of the hysteresis loop and the upper curve is the base branch from pH 2·8. Curves are for time-independent absorbance readings (see text).
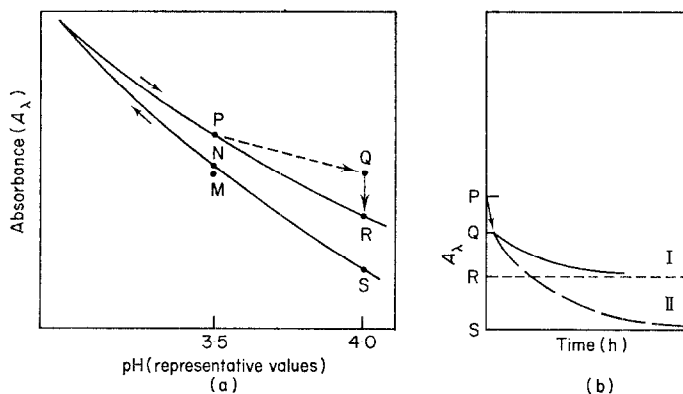
FIG. 4. Time-course of absorbance after a change in pH (schematic). See text for details.

resulting pH value is, say, 4·0. If we read the absorbance as soon as possible after adding the titrant, the A_λ value will be that of point Q. The absorbance then falls to point R over a period of several hours (the length of time depending on the actual pH and on the size of the pH change between points P and R). The time-course of the absorbance change is shown in Figure 4(b). With our experimental procedure we cannot follow the kinetics of the fast drop in absorbance from P to Q. We can, however, monitor the levelling-off of the absorbance change to point R (curve I, Fig. 4(b)). We shall consider below the nature of the reaction which results in the slow change in A_λ from Q to R.

The points from which Figure 2(a) to (f) were constructed are "levelled-off" values, and it is in this sense that the hysteresis loops are time independent. Leaving the solution for an additional 24 hours or more at point R on the base branch does not result in significant further decrease of the absorbance. (It was not feasible to leave the solutions for weeks or months due to degradation by hydrolysis or from any nucleases which may have slipped through despite our precautions (Cox, 1968).)

If we consider the addition of acid to a solution at point S on the acid branch of the loop (Fig. 4(a)), we find similar temporal behavior. Our first A_λ reading after adding the acid is at point M, and the absorbance slowly rises to a final value at point N. The absorbance difference represented by points NM was found to be rather smaller than that represented by points QR (the value for NM was typically $\leq 0·005$ absorbance unit for $[P] = 10^{-4}$ M), and A_λ levels off at N after one to two hours.

Although there are slow absorbance changes with time after addition of a portion of titrant, the "time-independent" values (cf. R, N) are independent of the rate of titration used in reaching these values. Thus, the curves in Figure 2 were first derived from several very slow titrations; each pH change was 0·25 unit and no titrant was added until the absorbance change had levelled off (2 to 8 h at each pH value). Such long titrations were not very practical if, for instance, pairs of solutions were desired at the same pH value but on different branches of the loop. Therefore, experiments were performed in which solutions were titrated to low pH rather quickly (reading absorbance every 0·5 pH unit and waiting only 5 to 10 min at each pH) and were then titrated with base directly to the pH value of interest. When the slow absorbance changes at this pH ceased after some hours, it was found that the final absorbance

readings were the same (within a small scatter) as those from the very slow titrations. Thus, any slow reactions which may be occurring at lower pH values do not affect the time-independent base branch of the hysteresis loop. It was likewise found that the time-independent values of absorbance for the acid branch also do not depend on the titration rate.

The situation at low ionic strength appears to be less complex, since any slow changes in absorbance following addition of acid or base were found to be quite small.

(d) *Dependence of hysteresis loops on ionic strength and ionic composition*

Most experiments were performed using solutions of RNA in 0·1 M-Na$^+$ buffer, containing 0·099 M-NaCl and 0·001 M-sodium cacodylate. The absence of cacodylate had no effect on the titration curves. Some titrations were made using solutions of RNA in 0·1 M-Na$^+$ buffer to which either Mg^{2+} ions ($\sim 2 \times 10^{-4}$ M) or EDTA ($\sim 5 \times 10^{-4}$ M) had been added. These experiments yielded two very important results.

(1) The acid branch titration curves (at $I = 0·1$ M) were found to be identical for experiments using buffers containing NaCl only, or to which Mg^{2+} ions or EDTA had been added. Thus, the presence or absence of Mg^{2+} ions does not appear to affect the changes in secondary structure which occur as the pH is lowered from pH 7.

(2) In contrast, the base branch of the hysteresis cycle is markedly affected by Mg^{2+} ions. *The complexing of divalent ions by EDTA eliminates the hysteresis.* In solutions containing EDTA, we still observed slow changes in absorbance after the pH was raised by addition of base, but the "levelled-off" value of A_λ coincided with the acid branch. This situation is illustrated by curve II of Figure 4(b). After the pH was changed from, typically, 3·5 to 4·0, our first absorbance reading was, say, at point Q. The value of A_λ then decreased with time along curve II, eventually (after several hours) reaching a final, time-independent value at point S, which lies on the acid branch of the hysteresis loop. (Note that curves I and II in Figure 4(b) are for illustrative purposes only—no quantitative significance should be attached to the relative rates of absorbance decrease shown in these curves.) Thus, the presence of Mg^{2+} ions seems to be necessary for formation and retention of at least some of the metastable conformations which rRNA may assume.

Support for these conclusions derives from the observation that addition of excess EDTA to a solution at pH 4 on the acid branch results in no change in the (dilution-corrected) absorbance. A slow decrease in A_λ (over a 24-hour period) is seen for the corresponding base branch solution plus EDTA, with the levelled-off value being somewhat above the acid-branch value. This implies that EDTA can remove some, but not all, of the Mg^{2+} ions tightly bound to base-branch RNA.

Titrations in the presence of Mg^{2+} gave hysteresis loops as shown in Figure 2. In the absence of either additional Mg^{2+} or EDTA, loops identical to those in Figure 2 were found upon titration of our first RNA preparation, while smaller loops were obtained using a second preparation of RNA. We conclude that the first RNA batch may have contained enough residual Mg^{2+} to give the full loops, while the second preparation had a lower level of residual Mg^{2+}.
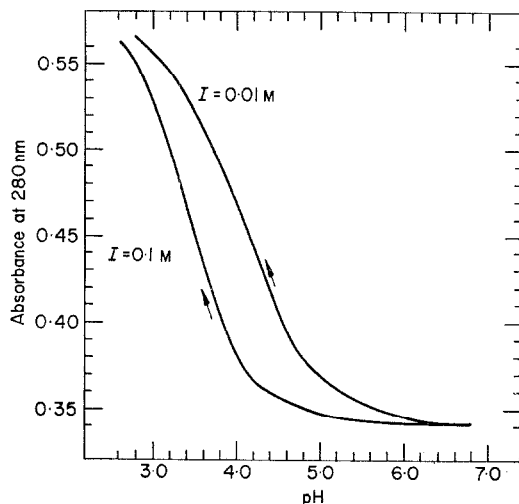
FIG. 5. Comparison of acid-branch titration curves at $T = 20°C$ for solutions of different ionic strength. Data were converted to the standard RNA concentration of 10^{-4} M-[P].

A decrease in ionic strength to 0·01 M (0·009 M-NaCl, 0·001 M-sodium cacodylate) has a marked effect. Comparing the acid titration curves at $\lambda = 280$ nm for $I = 0·1$ M and $I = 0·01$ M solutions (Fig. 5) we see that, as expected, the higher salt concentration retards the opening of the RNA structure, which occurs at much higher pH values in the $I = 0·01$ M solution (Cox & Littauer, 1963). Furthermore, the hysteresis virtually disappears at low ionic strength (Fig. 3). It is found that the titration curve is rapidly reversible between pH 2·8 and pH 4. That is, in this pH range our first A_λ reading after addition of base was coincident with the acid-branch curve, and we observed no further decrease in absorbance with time. There does appear to be a small hysteresis as shown in Figure 3. It should be noted that the ionic strength increases during the titration cycle due to addition of titrant, as well as from diffusion of KCl from the reference electrode tip. This last effect can be quite important—when, as a test, we left the electrode in pH 7 RNA solution for two days before commencing the titration, a curve was obtained intermediate to those shown in Figure 5. The results in Figure 3 are from fairly rapid titration experiments (cycle time about 3 hours). In any case, we see that the hysteresis becomes less pronounced at lower ionic strength.

(e) Intramolecular nature of hysteresis

Direct evidence that the hysteresis phenomenon reflects intramolecular conformational rearrangements is provided by ultracentrifuge measurements. Sedimentation coefficients measured at several pH values (Revzin et al., manuscript in preparation) do not show large variation with pH down to about pH 3, and certainly do not indicate even aggregation to dimers. Additional evidence against aggregation is derived from analysis of the sedimentation boundaries. At each pH value, a well-defined two-peak system was observed, as expected for our 16 S and 23 S mixture of rRNA.

As a further check, solutions were prepared at pH 3·7 on the acid and base branches (at $I = 0.1$ M), and a sedimentation run was performed on both solutions simultaneously. The results are shown in Table 1.

TABLE 1

Sedimentation coefficients at pH 3·7

Solution	s_{fast}	s_{slow}
Acid branch	20·5 S	15·5 S
Base branch	21·5 S	16·5 S

RNA concentration $= 10^{-4}$ M-[P], $T = 20°C$, $I = 0.1$ M.

Each solution showed a two-peak sedimentation boundary. The s-values for the base-branch are seen to be slightly larger than those for the acid-branch solution. This similarity in s values for the two branches appears to exclude the possibility that appreciable intermolecular association is involved in the hysteresis effects.

Titration experiments at different RNA concentrations can also give information about any possible aggregation. Our experimental set-up did not permit variation of the nucleotide concentration over a wide range, but spectrophotometric results from solutions differing in [P] concentration by a factor of two gave identical titration curves (after conversion of the data to the "standard concentration", 10^{-4} M-[P], Fig. 2). It is also worth noting that hysteresis is observed both optically and potentiometrically, although the RNA concentration in the absorbance experiments is lower by a factor of 40.

Absorbance readings at $\lambda = 340$ nm were taken for each pH value in the spectrophotometric titrations. RNA shows virtually no absorbance at this wavelength, so changes in A_{340} can be attributed to scattering from large aggregates which might possibly form. The value of A_{340} was less than 0·005 unit and was invariant over the entire pH range, indicating the absence of large aggregated particles. We also measured A_{340} as a function of pH for an RNA solution having [P] $= 4 \times 10^{-3}$ M (comparable to the concentrations used in proton-binding experiments). The value of A_{340} was unaffected by titration to pH 3. No change was observed even after 12 hours, nor was any precipitate seen visually in this experiment or at any time during any of the potentiometric titrations. In summary, then, we may seek an explanation for the hysteresis phenomenon in terms of the presence of metastable secondary structures in single rRNA molecules.

(f) Hysteresis cycles at 30°C and at 35°C

Slow optical titrations were performed at 30°C and at 35°C, in which each change in pH was 0·25 unit and no acid or base was added until the absorbance changes occurring after the previous addition of titrant had levelled off. The time-independent hysteresis loops were found to be similar to those at 20°C, as given in Figure 2. (The higher temperature loops are translated to higher pH by <0·5 pH unit.) Thus, the higher temperatures used apparently do not markedly affect the formation of those

structures upon which the hysteresis is based. The rates of the slow absorbance changes on the base branch increase with higher temperature, with levelling off completed in one to two hours.

(g) Kinetics of the slow processes occurring after addition of titrant

The kinetics of the slow processes on both the acid and base branches were followed by reading the absorbance at various times during the levelling off period (cf. curve I, Fig. 4(b)). The small total changes in A_λ for points on the acid branch did not allow quantitative analysis of the rates. The effects were larger for the base branch and thus were more amenable to analysis. It seemed most likely that the slow changes on the base-branch result from "annealing" (by slippage) of mismatched base-paired regions to more stable configurations. Annealing reactions with half-lives of up to several days (at room temperature) have been observed for long-chain synthetic poly-nucleotides (Blake & Fresco, 1966; M. Spodheim, unpublished data) and for d(A-T) oligomers (Scheffler et al., 1968; Baldwin, 1968).

A single annealing process should follow an apparent first-order rate law. The experimental quantities are the absorbance readings at times zero (A_0), t (A_t), and infinity (levelled-off value, A_∞); thus a plot of log $[(A_t - A_\infty)]/[(A_0 - A_\infty)]$ versus t should give a straight line having slope $-(2\cdot3\tau)^{-1}$, where τ is the relaxation time for the process.
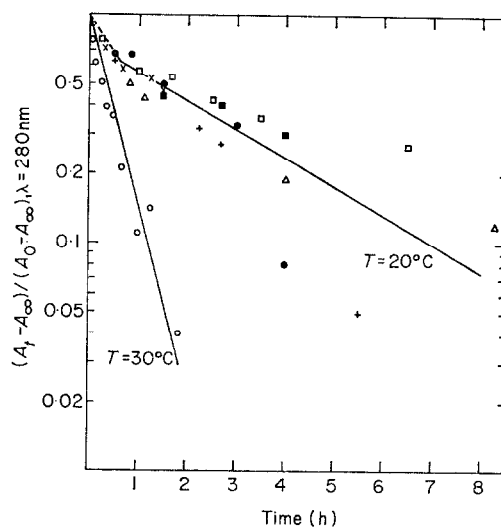

FIG. 6. Evaluation of kinetic data at pH 4·25 for slow absorbance changes on the base branch $(I = 0\cdot1$ M solution), see text. Symbols ($\square$), ($\blacksquare$), ($\times$), ($+$), ($\bullet$), ($\triangle$) are for experiments at $T = 20°C$; symbol ($\bigcirc$) is for $T = 30°C$. For all data shown, the pH had been increased from pH 3·5 to pH 4·25, at which pH the absorbance changes were recorded as functions of time.

Figure 6 is such a graph for data at pH 4·25, $I = 0\cdot1$ M. It can be seen that straight lines are found within the scatter of the data. Although the scatter is large enough to preclude detailed consideration of other reaction orders, the data do imply that the slow process, on average, follows a first-order kinetic law. Using Figure 6, then, we find $\tau_1^{-1} \simeq 0\cdot3$ h^{-1} at 20°C, and $\tau_2^{-1} \simeq 1\cdot9$ h^{-1} at 30°C. The slippage mechanism

probably requires that an entire sequence of base pairs open up before annealing to a more stable structure can occur. The value of τ^{-1} should primarily reflect the rate of this slow dissociation step. Thus, we may write $\tau^{-1} = k_d$, where k_d denotes the average apparent rate constant for the dissociation. In such a case, we may use the change in relaxation time with temperature to estimate the average activation energy, E_a, for the dissociation process, and we find $E_a \simeq 32$ kcal/mol.

These rough values for τ^{-1} and E_a indicate the magnitudes of the quantities involved. The long relaxation times and rather high activation energy imply that the process under consideration involves a large number of elementary steps. The kinetic data for other pH values generally gave similar results, although in some cases relaxation times at 20°C and at 30°C were more nearly equal, indicating a lower activation energy at these pH values. We cannot predict *a priori* the changes in τ^{-1} and E_a with pH or temperature, since the exact reaction mechanism and the average stability for all mismatched regions may vary with pH. A more complete kinetic study could reveal details about these mismatched "short-lived" metastable states that can form at acidic pH values. For the time being we note that our kinetic data are consistent with the interpretation that the slow process observed on the base branch is an annealing by slippage reaction.

(h) *Absorbance difference spectra at 80°C*

Solutions at the same pH but on different branches of the hysteresis loop were heated to 75 to 85°C. We wished to observe whether the metastable structures that are present at 20°C break down at higher temperatures, with *both* solutions then reverting to the "equilibrium" state upon cooling. If, on the other hand, some metastable conformations persist at 80°C, we may use the spectral differences between the acid and base-branch solutions (at 80°C) to deduce the nature of the metastable structures themselves.

We find that heating to 80°C does not destroy the metastable conformations in Mg^{2+}-containing solutions; the differences between the acid and base branches are reproduced at all λ after the solutions are cooled back to 20°C. Heating to 80°C does seem to cause some hydrolytic degradation of the RNA, but the small absorbance increase accompanying the hydrolysis is very nearly the same for both branches. In some experiments the spectral differences at 20°C before and after heating were similar but not quite identical. This may be due to some experimental uncertainties or to breakdown of a fairly small fraction of the metastable states at high temperature. In general, however, we conclude that heating to 80°C in the presence of Mg^{2+} ions does not cause the system to overcome the high energy barrier that gives rise to the long-lived metastability. On the other hand, heating of acid and base-branch solutions to which excess EDTA was added gave equal absorbance values at 60°C and at 80°C, and furthermore the absorbance spectra remained coincident after cooling to 20°C.

Spectral differences at 20°C between iso-pH solutions on the two branches of the hysteresis loop are due not only to the specific structures that are responsible for the metastability, but also include contributions from other structures (cf. $A \cdot U$ and $G \cdot C$ base pairs) which may be prevented from forming (or are induced to form) because of the presence of the metastable conformations. The same problem exists when comparing spectra at high temperature, but to a much lesser extent since at 80°C most
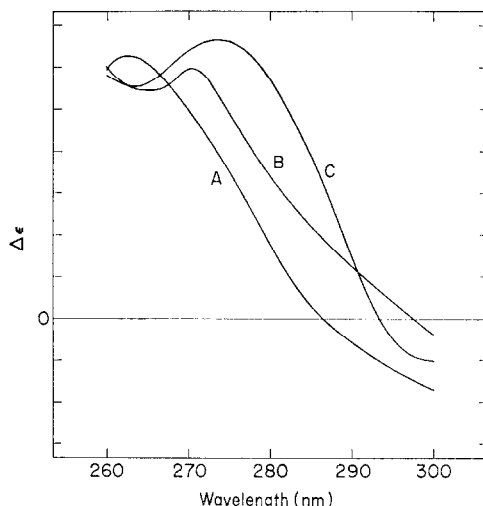
FIG. 7. Absorbance difference spectra (in arbitrary units) at $T = 80°C$, for iso-pH solutions on the two branches of the hysteresis loop. Curve A, pH 4·0; curve B, pH 3·7. In both cases, at 80°C the absorbance of the base-branch solution is lower than that of the acid-branch solution. Curve C represents absorbance changes upon formation of G·G helical structures (Pochon & Michelson, 1965). Protonation of G·G base pairs will have little effect on the shape of curve C (Beaven *et al.*, 1955). If curve C is modified to include spectral changes accompanying A·A formation (Revzin *et al.*, manuscript in preparation) the resulting curve will more closely resemble the experimental curves A and B.

of the extraneous structures have melted out (Stanley & Bock, 1965; Cox, 1966). The major part of the difference spectrum at 80°C may thus arise from the metastable structure itself. Accordingly, we have evaluated the difference spectra at 80°C for solutions at pH 3·7 and at pH 4·0 (Fig. 7). We wish first to emphasize the result that, while at 20°C the absorbance on the base branch is higher (indicating less structure than on the acid branch), this situation is reversed at elevated temperature, where we find that there is a lower absorbance (and hence more structure) for the base branch. We see from curves A and B in Figure 7 that difference spectra at both pH values have the same general shape. Comparison of curves A and B in Figure 7 with spectra for various conceivable metastable conformations shows that spectral differences at 80°C are consistent with the presence of protonated G·G structures in RNA on the base branch (curve C of Fig. 7) (Beaven *et al.*, 1955; Pochon & Michelson, 1965). It is of further interest that the presence of protonated A·A base pairs in addition to G·G pairs in the metastable conformation could shift the predicted curve C into closer agreement with the experimental results curve A and curve B (Revzin *et al.*, manuscript in preparation).

(i) *Titration of transfer RNA*

Spectrophotometric titration of a preparation of unfractionated *E. coli* tRNAs showed no time-independent hysteresis loops (Fig. 8). Slow changes in absorbance with time following addition of acid were very small or non-existent. However, slow changes with time were noted upon titration with base. These changes, which as in rRNA are presumably due to annealing of mismatched regions, appeared to level off after about one hour, with the final (dilution corrected) absorbance value being the
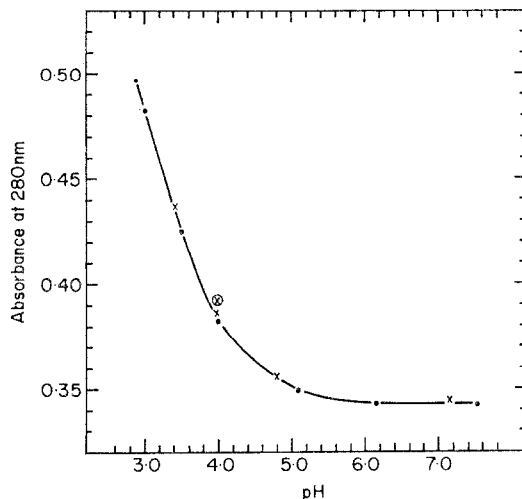
Fig. 8. Spectrophotometric titration of unfractionated *E. coli* tRNA. Experimental conditions: $T = 20°C$; buffer, 0·099 M-NaCl, 0·001 M-sodium cacodylate, $\sim 2 \times 10^{-4}$ M-MgCl$_2$; tRNA concentration, $\sim 10^{-4}$ M-[P]. Symbols (●) are time-independent values upon titration with acid from pH 7, symbols (×) are time-independent values upon titration with base from pH 2·8. At pH 4, (⊗) is the first absorbance reading following the pH change from pH 3·4, while (×) is the levelled-off reading coincident with the acid branch.

same as that on the acid branch. Thus, a tRNA mixture can pass through "short-lived" metastable conformational states, but does not show a long-lived hysteresis phenomenon as does ribosomal RNA.

4. Discussion

(a) *Events that occur during the RNA titration cycle*

We note again our assumption that the pH 7 structure corresponds to the generally accepted model for rRNA; namely, that the molecule is composed of a series of double-helical regions (stabilized primarily by Watson–Crick base pairs) connected by single-stranded lengths of unpaired bases. As the pH of an RNA solution of 0·1 M ionic strength is lowered, a number of reactions occur, including the protonation of A, C and G residues, along with the opening of A·U and G·C base pairs (Cox & Littauer, 1963). A detailed analysis of absorbance and proton-binding data (Revzin *et al.*, manuscript in preparation) implies that in addition to the above-mentioned processes some other reactions also take place. One of these reactions may be the formation of a protonated three-stranded G·C·G structure in the region $3\cdot8 < \text{pH} < 6\cdot0$. This structure disappears at lower pH, and conformations consisting of sequences rich in G·G and A·A double helices may be formed. We believe that the "high pH" structure is not very important for the hysteresis, but that the second class of structures is crucial. The extent of "low pH" structure formation increases as the pH approaches pH 2·6. Upon addition of base, the acid-stable regions are eventually transformed to the various structures which are present at higher pH, but these reverse processes set in at pH values considerably above those at which the forward reactions take place. This, of course, is merely a statement that hysteresis is displayed by the system.

(b) *The acid branch of the hysteresis cycle is an equilibrium curve*

In general, both branches of a hysteresis cycle can represent metastable states of the system—the true equilibrium curve would then lie somewhere within the loop (Everett, 1967). For RNA, the titrations in EDTA solution show that in the absence of Mg^{2+} the system does not display hysteresis. Rather the same time-independent curve is followed whether the pH is being decreased or increased, and this curve coincides with the acid branch of the hysteresis loop in Mg^{2+} solution. Removal of Mg^{2+} ions from the base-branch solution using EDTA (plus heat) also causes the system to relax to the acid-branch curve. Thus, the acid branch is the equilibrium curve and the metastable states (in Mg^{2+} solution) occur along the base branch. The changes in secondary structure that occur upon titration with acid are apparently identical in the presence or absence of Mg^{2+}. Therefore, the non-equilibrium structure is most probably an acid-stable conformation (either $G \cdot C \cdot G$ or ($G \cdot G$, $A \cdot A$)) which is "frozen" by Mg^{2+} ions into a metastable state.

The proposed triple-helical structure begins to form at about pH 6, yet the hysteresis is seen only if the pH has been decreased below pH 3·8. Thus the high pH structure does not appear to be responsible for the metastability. In general, it is assumed that a metastable state is prevented from transforming to the equilibrium state (of lower free energy) by the presence of a large energy barrier. It seems unlikely that such an energy barrier would suddenly develop in the high pH structure as the pH is lowered below pH 3·8.

(c) *Metastable guanine·guanine structures may underlie the hysteresis*

A number of observations has led us to conclude that $G \cdot G$ structures are present in metastable conformation on the base branch of the cycle. The absorbance difference spectra at 80°C for iso-pH RNA solutions at pH 3·7 and at pH 4·0 are consistent with the presence of $G \cdot G$ rich sequences in RNA on the base branch even though we predict that such sequences are not present at these pH values on the acid branch. Thus, $G \cdot G$ rich regions which form only at lower pH on the acid branch appear to persist to higher pH values on the base branch. The high stability of $G \cdot G$ structures is well known (for review see Michelson *et al.*, 1967; Fresco & Massoulié, 1963; Pochon & Michelson, 1965). For example, to prepare poly(G)·poly(C) by mixing poly(G) and poly(C), it is necessary to heat the solution to at least 80°C (in 8 M-urea) (Englander *et al.*, 1972). Thus, even in the presence of the poly(C), which creates a large driving force for formation of the very stable poly(G)·poly(C) structure, poly(G) persists in metastable, self-associated conformations to rather high temperatures. Guanine residues can aggregate into a number of structures, involving several possible base pairing schemes (Gellert *et al.*, 1962; Pochon & Michelson, 1965; Chantot *et al.*, 1971). One can devise $G \cdot G$ base pairs in which protons participate in H bonding and are thus essential for the $G \cdot G$ formation. One can also propose $G \cdot G$ pairings in which protons merely help to stabilize the structure by partially compensating the electrostatic repulsion between the negatively charged phosphate backbones. The strands of $G \cdot G$ helices might be parallel or antiparallel. We conclude, therefore, that the versatility of G residues in forming helical structures, some (or all) of which are known to show metastability, coupled with our prediction that $G \cdot G$ is formed at low pH on the acid branch (Revzin *et al.*, manuscript in preparation) and with the difference spectra at

80°C provides strong support for our contention that G·G regions have an important role in causing the hysteresis.

We have observed that Mg^{2+} ions can convert a structure that is not metastable in the presence of EDTA into a metastable conformation. Similar marked effects of Mg^{2+} ions are well known from other studies of polynucleotides. For example, a 1:1 mixture of poly(A) and poly(U) ([P] $\sim 10^{-4}$ M) in NaCl solution will form a complex only when the Na^+ ion concentration is at least 10^{-2} M. In $MgCl_2$ solution, however, the complex will form when the Mg^{2+} ion concentration is only 10^{-4} M— a factor of 100 lower than for the solution of monovalent cations (Felsenfeld & Rich, 1957). Even more relevant to our study is the finding of Fresco and co-workers (Lindahl et al., 1966; Adams et al., 1967) that certain tRNAs can exist in more than one form at room temperature, depending on whether Mg^{2+} ions are present in the system. In one such "denaturable" tRNA system, interconversion between the two forms is achieved by heating to 60°C in the presence of Mg^{2+} (Lindahl et al., 1966). Our hysteresis results give further evidence that Mg^{2+} ions can have a unique role in stabilizing multi-stranded polynucleotide conformations.

It is observed experimentally that there is little or no hysteresis in solutions of 0·01 M ionic strength. We have concluded from our quantitative analysis of absorbance data (Revzin et al., manuscript in preparation) that no triple-helices are formed at $I = 0·01$ M, but that G·G and A·A rich regions begin to form even at rather high pH values. This might be taken as indirect evidence that a metastable G·C·G structure is involved in the $I = 0·1$ M hysteresis. A more likely possibility, however, is that at lower ionic strength the increased electrostatic repulsion between the phosphate backbones prevents the triple helix from forming and also removes the metastability from the G·G regions so that these form and dissociate reasonably rapidly. Low ionic strength is known to stabilize some protonated polynucleotide structures, such as A·A and C·C (see Michelson et al., 1967, p. 102). However, even though the proposed G·C·G and G·G structures will involve protonated bases at low pH values, a decrease in ionic strength will stabilize such structures only if the proton provides a *net* attractive force for the phosphate–H^+–phosphate system. We have no evidence that this need be the case for our proposed helical regions, which could well be destabilized at lower ionic strengths.

We have presented evidence that G·G along with A·A base pairs may be involved in metastable structures during the titration cycle of ribosomal RNA. In sequencing *E. coli* rRNA, Fellner and his associates have found certain rather long sequences (up to 17 residues) containing only G and A, except for one or two pyrimidine residues (Fellner et al., 1972a,b; Ehresmann et al., 1972). Furthermore, there are several homologous sequences rich in G and A residues. Should two such sequences match up during titration, they could be very stable, since any A·A base pairs would help stabilize the structure, especially if the strands are parallel. Our tRNA titrations imply that the sequences that underlie the hysteresis in rRNA may be rather long ones. The mixture of tRNAs should approximate a ribosomal RNA in that the double-helical regions present at pH 7 will vary in base composition from mostly A·U to mostly G·C, although the tRNAs sequenced to date seem to have helical regions of limited length (4 to 7 base pairs). There are apparently few long stretches of (A,G) residues (Zachau, 1969). Thus, the absence of hysteresis in the titration of unfractionated *E. coli* tRNA is indirect evidence that long purine stretches may underlie the long-lived metastability in rRNA.

The presence of metastable G·G structures at pH <3·8 is sufficient to account for the scanning curves from both branches of the cycle. The series of scanning curves obtained from the acid branch may simply reflect the formation of more G·G regions at lower pH values as additional G residues become available after the opening of A·U and G·C base pairs. These G·G regions break down only at a pH higher than the pH at which they are formed. However, once they do open up they are not re-formed until lower pH values; thus we have scanning from the base branch as well.

(d) Biological implications of metastable structures

Hysteresis phenomena that are familiar from physics, such as magnetic and ferro-electric hysteresis, are based on interactions among "domains" of polycrystalline systems (Everett, 1967). Ribosomal RNA presents an analogous situation, except that the "domains" are part of the same molecule. We can ask whether metastable conformational states in individual molecules may have a biological role. Katchalsky and co-workers (Katchalsky & Oplatka, 1966; Katchalsky & Neumann, 1972) have considered some aspects of this question.

We wish first to emphasize the importance of the time scale on which the lifetime of the metastability is considered. In general, time-independent hysteresis loops are taken to mean loops that do not change for days, weeks or months. For biological systems, such long lifetimes are probably not necessary, since a metastable structure that exists for several hours should be able to fulfil its designated function. Thus, the metastable conformations on the base branch of the rRNA hysteresis loop (or perhaps even the "short-lived" metastable states of the base branch which anneal out after hours) are probably "time independent" on a metabolic time scale.

We have studied ribosomal RNA, but, unfortunately, the mechanisms of ribosome function are so little understood that we can only state generalities such as "meta-stable conformations of ribosomes could affect protein synthesis". It is worthy of note that Fukami & Imahori (1971) have induced metastable states in R17 viral RNA used as a messenger RNA, and have observed different rates of protein synthe-sis for the native and denatured forms. Likewise, it has been speculated that the denaturable tRNAs discovered by Fresco et al. (1966) and by Gartland & Sueoka (1966) could also have a role in the protein synthesis control mechanism. An impor-tant feature of the metastable state is that, should such a structure be generated during a singular cellular event (e.g. a nerve impulse or a sudden ion flux), it will remain in the metastable conformation even though the environment has returned to "normal" after the event. Thus, metastable states may influence biological pro-cesses long after the initial trigger signal has passed.

5. Conclusion

The existence of hysteresis in the titration behaviour of E. coli rRNA has led us to delve into the structures and the kinetic barriers that exist in ribosomal RNA mole-cules at the various stages of the titration cycle. We propose that metastable G·G structures are involved in the hysteresis phenomenon. We conclude that the possibi-lity of metastable conformations involving G residues may be worth considering when examining the properties of all natural RNAs which display marked secondary structure.

8

REFERENCES

Adams, A., Lindahl, T. & Fresco, J. R. (1967). *Proc. Nat. Acad. Sci., U.S.A.* **57**, 1684–1691.

Arnott, S., Hutchinson, F., Spencer, M., Wilkins, M. H. F., Fuller, W. & Langridge, R. (1966). *Nature (London)*, **211**, 227–232.

Baldwin, R. L. (1968). In *Molecular Associations in Biology* (Pullman, B., ed.), pp. 145–162, Academic Press, New York.

Beaven, G. H., Holiday, E. R. & Johnson, E. A. (1955). In *The Nucleic Acids* (Chargaff, E. & Davidson, J. N., eds), vol. 1, pp. 493–553, Academic Press, New York.

Blake, R. D. & Fresco, J. R. (1966). *J. Mol. Biol.* **19**, 145–160.

Chantot, J. F., Sarocchi, M. Th. & Guschlbauer, W. (1971). *Biochimie*, **53**, 347–354.

Cox, R. A. (1966). *Biochem. J.* **98**, 841–857.

Cox, R. A. (1968). *Quart. Rev. Chem. Soc.* **22**, 499–526.

Cox, R. A. & Katchalsky, A. (1972). *Biochem. J.* **126**, 1039–1054.

Cox, R. A. & Littauer, U. Z. (1963). *Biochim. Biophys. Acta*, **72**, 188–202.

Doty, P., Boedtker, H., Fresco, J. R., Haselkorn, R. & Litt, M. (1959). *Proc. Nat. Acad. Sci., U.S.A.* **45**, 482–499.

Ehresmann, C., Stiegler, P., Fellner, P. & Ebel, J.-P. (1972). *Biochimie*, **54**, 901–967.

Eilam, Y. & Elson, D. (1971). *Biochemistry*, **10**, 1489–1495.

Englander, J. J., Kallenbach, N. R. & Englander, S. W. (1972). *J. Mol. Biol.* **63**, 153–169.

Everett, D. H. (1967). In *The Solid–Gas Interface* (Flood, E. A., ed.), vol. 2, pp. 1055–1113, Marcel Dekker, New York.

Fellner, P., Ehresmann, C. & Ebel, J.-P. (1972a). *Biochimie*, **54**, 853–900.

Fellner, P., Ehresmann, C., Stiegler, P. & Ebel, J.-P. (1972b). *Nature New Biol.* **239**, 1–5.

Felsenfeld, G. & Rich, A. (1957). *Biochim. Biophys. Acta*, **26**, 457–468.

Fresco, J. R. & Massoulié, J. (1963). *J. Amer. Chem. Soc.* **85**, 1352–1353.

Fresco, J. R., Adams, A., Ascione, R., Henley, D. & Lindahl, T. (1966). *Cold Spring Harbor Symp. Quant. Biol.* **31**, 527–537.

Fukami, H. & Imahori, K. (1971). *Proc. Nat. Acad. Sci., U.S.A.* **68**, 570–573.

Gartland, W. J. & Sueoka, N. (1966). *Proc. Nat. Acad. Sci., U.S.A.* **55**, 948–956.

Gellert, M., Lipsett, M. N. & Davies, D. R. (1962). *Proc. Nat. Acad. Sci., U.S.A.* **48**, 2013–2018.

Katchalsky, A. & Neumann, E. (1972). *Intern. J. Neuroscience*, **3**, 175–182.

Katchalsky, A. & Oplatka, A. (1966). *Neurosciences Res. Symp. Sum.* **1**, 352–374.

Lindahl, T., Adams, A. & Fresco, J. R. (1966). *Proc. Nat. Acad. Sci., U.S.A.* **55**, 941–948.

Littauer, U. Z. & Eisenberg, H. (1959). *Biochim. Biophys. Acta*, **32**, 320–337.

Michelson, A. M., Massoulié, J. & Guschlbauer, W. (1967). *Progr. Nucl. Acid Res. Mol. Biol.* **6**, 83–141.

Pochon, F. & Michelson, A. M. (1965). *Proc. Nat. Acad. Sci., U.S.A.* **53**, 1425–1430.

Scheffler, I. E., Elson, E. L. & Baldwin, R. L. (1968). *J. Mol. Biol.* **36**, 291–304.

Spirin, A. S. & Gavrilova, L. P. (1969). *The Ribosome*, Springer-Verlag, Berlin.

Spitnik-Elson, P. & Atsmon, A. (1969). *J. Mol. Biol.* **45**, 113–124.

Stanley, W. M., Jr. & Bock, R. M. (1965). *Biochemistry*, **4**, 1302–1311.

Steinhardt, J. & Beychock, S. (1964). In *The Proteins* (Neurath, H., ed.), vol. 2, 2nd edit., pp. 139–304, Academic Press, New York.

Tanford, C. (1962). *Advan. Protein Chem.* **17**, 69–165.

Timasheff, S. N., Witz, J. & Luzzati, V. (1961). *Biophys. J.* **1**, 525–537.

Zachau, H. G. (1969). *Angew. Chem. Internat. Edit.* **8**, 711–727.